
Discrete Message via Online Clustering Labels in Decentralized POMDP

Jingdi Chen

The George Washington University
Washington, DC 20052
jingdic@gwu.edu

Tian Lan

The George Washington University
Washington, DC 20052
tlan@gwu.edu

Abstract

Communication is crucial for solving cooperative Multi-Agent Reinforcement Learning tasks in Partially-Observable Markov Decision Processes. Existing works often rely on black-box methods to encode local information/features into messages shared with other agents. However, such black-box approaches are unable to provide any quantitative guarantees on the expected return and often lead to the generation of continuous messages with high communication overhead and poor interpretability. In this paper, we establish an upper bound on the return gap between an ideal policy with full observability and an optimal partially-observable policy with discrete communication. This result enables us to recast multi-agent communication into a novel online clustering problem over the local observations at each agent, with messages as cluster labels and the upper bound on the return gap as clustering loss. By minimizing the upper bound, we propose a surprisingly simple design of message generation functions in multi-agent communication and integrate it with reinforcement learning using a Regularized Information Maximization loss function. Evaluations show that the proposed discrete communication significantly outperforms state-of-the-art multi-agent communication baselines and can achieve nearly-optimal returns with few-bit messages that are naturally interpretable. Codes are available at: <https://anonymous.4open.science/r/RGMComm-72AC/>.

1 Introduction

Multi-Agent Reinforcement Learning (MARL) has succeeded in complex tasks [1, 2], but decentralized policies limit performance in Partially Observable Markov Decision Process (POMDP) problems, where agents have limited views of the environment [3]. Communication is crucial for decentralized decision-making. Existing approaches consider *what*[4–8] and *who*[9, 10] to communicate. However, communication messages are often generated by directly encoding local information/features with Deep Neural Networks (DNN) or attention networks, as guided by some mutual information loss [11–14]. These are largely black-box approaches without any quantitative guarantees on the expected return and offers little explainability of the messages [15]. Since messages drawn from a continuous space are real-valued and may incur high communication overhead, existing works have considered communication with discrete messages [6, 5, 16, 17, 3], but again provide no average return guarantees for POMDP with communication.

In this paper, we propose a discrete MARL communication framework that achieves a closed-form guarantee on the optimal expected average return for Partially Observable Markov Decision Processes (POMDPs). The framework analyzes the relevant information in each agent’s local observations for other agents’ decision-making and supports message sharing using a finite-size discrete alphabet. More precisely, consider a problem with n agents. Each agent j computes a message m_{ij} for agent i based on its local observation o_j in each step t . Let $m_{-i} = \{m_{ij}, \forall j\}$ be the collection of all messages received by agent i . For any discrete communication strategies, we quantify the

gap between the optimal expected average return of an ideal policy with full observability, i.e., $\pi^* = [\pi_i^*(a_i|o_1, \dots, o_n), \forall i]$ and the optimal expected average return of a communication-enabled, partially-observable policy, i.e., $\pi = [\pi_i(a_i|o_i, m_{-i}), \forall i]$. Since minimizing the return gap directly is intractable, we derive a closed-form upper bound and minimize it to find the optimal communication strategy, which is a common technique in Machine Learning (ML) [18, 19]. Specifically, the upper bound is proven to be $O(\sqrt{\epsilon n Q_{\max}})$, where ϵ represents the average cosine-distance between joint action-value vectors corresponding to the same messages, n is the number of agents, and Q_{\max} is the highest action-value. The result inspires a communication framework based on an online clustering algorithm to minimize ϵ . Our key insight is that the problem of generating messages m_{ij} from local observations o_j can be viewed as an online clustering problem with o_j as inputs and m_{ij} as labels, with respect to a new loss function to minimize the return bound. Since the policy of agent i with communication is conditioned on local observation o_i and messages m_{-i} rather than the full observation o_1, \dots, o_n , its impact on optimal expected average return can be characterized using a Policy Change Lemma and relying on the average distance ϵ for corresponding joint action-values in each cluster. The messages generation problem thus is formulated as an online clustering problem, where local observations serve as inputs and messages as labels, using a new loss function. The proposed framework integrates with state-of-the-art MARL algorithms adopting Centralized Training Decentralized Execution (CTDE), e.g., MADDPG[5], QMIX[20], PAC[21], and DOP[22] that use joint action-values, and an online clustering algorithm with a Regularized Information Maximization (RIM) loss function is leveraged. The algorithm generates interpretable discrete messages and extends to MARL problems with continuous state space using replay buffer sampling. Evaluations on continuous state space problems demonstrate significant improvements over existing communication-enabled MARL algorithms, including CommNet[7], MADDPG[5], IC3Net [23], TarMAC[9], and SARNet [10]. Our contributions include the proposal of a discrete communication framework, the quantification of the return gap with a closed-form upper bound, and the introduction of a new class of MARL communication algorithms that achieve nearly-optimal returns with few-bit messages, outperforming state-of-the-art baselines.

2 Related Work

Multi-Agent Reinforcement Learning (MARL): MARL [24–26] has gained significant attention in the field of Reinforcement Learning (RL). This paper focuses on cooperative MARL, which is typically modeled as a Decentralized Partially Observable Markov Decision Process (Dec-POMDP)[27], where all agents aim to maximize the long-term return by sharing a reward. The Centralized Training with Decentralized Execution (CTDE) paradigm[5] is widely used in cooperative MARL. Many MARL algorithms, including COMA [28], MAAC [29], VDN [30], QMIX [20], MD-MADDPG [31], FAC-MADDPG [32], MA-PPO [33], DOP [22], FOP [34], and PMIC [14], adopt CTDE paradigms to improve performance in cooperative MARL.

MARL with Communication: Communication in MARL has seen advancements in recent years. CommNet [7] and BiCNet [35] employ recurrent neural networks for communication, but suffer from information loss and high energy costs. IC3Net [23] and Gated-ACML [36] introduce gating mechanisms to determine when agents should send messages to others. TarMAC [9] utilizes multi-headed attention for information distribution, while ATOC [8] employs a bidirectional recurrent network. DICG [37] utilizes graph convolution, and SARNet [10] extends the structure of MD-MADDPG [31] and TarMAC [9] with query-key pairs of soft-attention. I2C [38] proposes communication only within an agent’s observation range, LSC [39] incorporates hierarchical communication structures through an auxiliary task. However, these approaches employ DNN as black-boxes, lacking interpretability due to their large parameter space [15, 40]. Additionally, previous protocols assume continuous real-valued messages, disregarding practical limitations of discrete communication networks with constrained information transfer rates. Some works assume discrete communication [6, 5, 16, 17, 3, 41–43], but lack policy regret minimization guarantees, operating as heuristic designs without performance guarantees.

3 Preliminaries and Problem Formulation

Dec-POMDP with communications: Decentralized partially-observable Markov decision process (Dec-POMDP) [27] models cooperative MARL where agents lack complete information on the

environment and have only local observations. Communication is crucial for strategy coordination in this scenario. It is a tuple $D = \langle S, A, P, \Omega, O, I, n, R, \gamma, g \rangle$, where S is the joint state space, $A = A_1 \times A_2 \times \dots \times A_n$ is the joint action space, where $\mathbf{a} = (a_1, a_2, \dots, a_n) \in A$ denotes the joint action of all agents. $P(s'|s, \mathbf{a}) : S \times A \times S \rightarrow [0, 1]$ is the transition function. Ω is the observation space. $O(s, i) : S \times I \rightarrow \Omega$ is a function that maps from the state space to distributions of observations for each agent i . $I = \{1, 2, \dots, n\}$ is a set of n agents, $R(s, \mathbf{a}) : S \times A \rightarrow \mathbb{R}$ is the reward function in terms of state s and joint action \mathbf{a} , γ the discount factor. g is the message generation function. We note that due to partial observability, the observation history of agent i , i.e., $o_i \in \mathcal{T}_i = (\Omega \times A_i)^t$ are often used to replace local observation o_i in formulating state- and action-value functions in POMDP [44–46]. For simplicity, we use a single notation o_i (and $\mathbf{o} = [o_1, \dots, o_n]$) nevertheless. Each agent i employs a message generation function $g(\mathbf{o}, i, j) : \Omega \times I \times I \rightarrow M$ to encode its local observation into a communication message for agent j . We use $m_{-i} = \{m_j = g(o_j), \forall j \neq i\}$ to denote the collection of messages agent i receives from all other agents $j \neq i$. In Dec-POMDP with communications, each agent i considers an individual policy $\pi_i(a_i|o_i, m_{-i})$ conditioned on local observation o_i and messages m_{-i} , i.e., $\pi = [\pi_i(a_i|o_i, m_{-i}), \forall i]$. To model the return gap, we also define an ideal policy with full observability: $\pi^* = [\pi_i^*(a_i|o_1, \dots, o_n), \forall i]$. In this paper, we assume the learning algorithm has access to all local observations during training as well as a joint action-value function (often represented using a DNN), but only its own observation and communication messages during execution.

Return Gap Minimization: Given a policy π , we consider the average expected return $J(\pi) = \lim_{T \rightarrow \infty} (1/T) \mathbb{E}_\pi[\sum_{t=0}^T R_t]$. The goal of this paper is to minimize the return gap between an ideal policy $\pi^* = [\pi_i^*(a_i|o_1, \dots, o_n), \forall i]$ with full observability and a partially-observable policy with communications $\pi = [\pi_i(a_i|o_i, m_{-i}), \forall i]$ where message labels $m_{-i} = \{m_j = g(o_j), \forall j \neq i\}$, i.e.,

$$\min J(\pi^*) - J(\pi, g). \quad (1)$$

While the problem is equivalent to maximizing $J(\pi, g)$, the return gap can indeed be analyzed more easily using Policy Change Lemma by contrasting π to π^* . It allows us to derive an upper bound of the return gap and enables design of efficient communication strategies to minimize the gap. We consider the discounted observation-based state value function and the corresponding action-value function for the Dec-POMDP:

$$V^\pi(\mathbf{o}) = \mathbb{E}_\pi\left[\sum_{i=0}^{\infty} \gamma^i \cdot R_{t+i} \mid \mathbf{o}_t = \mathbf{o}, \mathbf{a}_t \sim \pi\right], Q^\pi(\mathbf{o}, \mathbf{a}) = \mathbb{E}_\pi\left[\sum_{i=0}^{\infty} \gamma^i \cdot R_{t+i} \mid \mathbf{o}_t = \mathbf{o}, \mathbf{a}_t = \mathbf{a}\right]. \quad (2)$$

Re-writing the average expected return as the expectation over initial distribution in terms of $V^\pi(\mathbf{o})$:

$$J(\pi) = \lim_{\gamma \rightarrow 1} E_\mu[(1 - \gamma)V^\pi(\mathbf{o})]. \quad (3)$$

We will leverage this state-value function $V^\pi(\mathbf{o})$ and its corresponding action-value function $Q^\pi(\mathbf{o}, \mathbf{a})$ to unroll the Dec-POMDP and derive a closed-form upper-bound to quantify the return gap. For $V^\pi(\mathbf{o})$ and $Q^\pi(\mathbf{o}, \mathbf{a})$ we suppress g for simpler notations.

4 Method

4.1 Theory Results

Since directly minimizing the return gap is intractable, we prove that the return gap between ideal policy π^* with full observability and optimal communication-enabled policy π with partial observability is bounded by $O(\sqrt{\epsilon n} Q_{\max})$ with respect to average cosine-distance ϵ in each cluster and maximum action-value Q_{\max} in Thm. 4.3. The proof consists of the following major steps: (i). We characterize the change in optimal expected average return $J(\pi^*) - J(\pi, g)$ for any two policies π^* and π based on the joint action-values under π^* . The result is stated as a Policy Change Lemma 4.1. (ii). We apply Policy Change Lemma 4.1 to two policies $\pi_{(j)}^*$ and $\pi_{(j)}$, which are identical in the observability and policies of agents $i \neq j$, except for that agent j 's policy is conditioned on communication messages m_{ij} respectively. We derived Lemma 4.2 that allows us to quantify the impact of message-encoding agent j 's local observations, rather than having complete access to this information, on the optimal expected average return gap. (iii). Finally, we construct a sequence of policies by changing the conditioning on each o_j to m_{ij} , one at a time. This allows us to quantify the desired return gap between π^* with full observability and communication-enabled policy π in Thm. 4.3. For simplicity, we use V^* to represent V^{π^*} , and Q^* to represent Q^{π^*} . Due to space limitations, we only give a sketch below and provide the complete proofs in the Appendix.

Consider the Dec-POMDP defined in Sec 3, we assume that observation/action spaces are finite, i.e., $|O| < \infty$ and $|A| < \infty$. It is worth noting that this is a technical condition to simplify the proof. For Dec-POMDPs with continuous observation and action spaces, the results can be easily extended by considering cosine-distance between action-value functions and replacing summations with integrals, or consider sampling the action-value functions as an approximation.

Lemma 4.1. (*Policy Change Lemma.*) *For any two policies π^* and π , the optimal expected average return gap is bounded by:*

$$J(\pi^*) - J(\pi, g) \leq \sum_m \sum_{\mathbf{o} \sim m} [Q^*(\mathbf{o}, \mathbf{a}_t^{\pi^*}) - Q^\pi(\mathbf{o}, \mathbf{a}_t^\pi)] \cdot d_\mu^\pi(\mathbf{o}), \quad d_\mu^\pi(\mathbf{o}) = (1-\gamma) \sum_{t=0}^{\infty} \gamma^t \cdot P(\mathbf{o}_t = \mathbf{o} | \pi, \mu), \quad (4)$$

where $d_\mu^\pi(\mathbf{o})$ is the γ -discounted visitation probability under policy π and initial distribution μ , and $\sum_{\mathbf{o} \sim m}$ is a sum over all observations corresponding to the same message.

Proof. Our key idea is to leverage state value function $V^\pi(\mathbf{o})$ and its corresponding action value function $Q^\pi(\mathbf{o}, \mathbf{a})$ in Eq.(2) to unroll the Dec-POMDP from timestep $t = 0$ and onward. The detailed proof is provided in Appendix. \square

Next, viewing the message generation $m_{ij} = g(o_j)$ as a clustering problem with o_j as input and m_{ij} as labels, we bound the policy gap between $\pi_{(j)}^*$ and $\pi_{(j)}$, which are optimal policies conditioned on o_j and m_{ij} , using the average cosine-distance of action value vectors $\bar{Q}^*(o_j)$ corresponding to o_j in the same cluster and its cluster center $\bar{H}(m) = \sum_{o_j \sim m} \bar{d}_m(o_j) \cdot \bar{Q}^*(o_j)$ under each message m . We define the action value vector corresponding observation o_j , i.e.,

$$\bar{Q}^*(o_j) = [\bar{Q}^*(o_{-j}, o_j), \forall o_{-j}], \quad \tilde{Q}^*(o_{-j}, o_j) = [Q^*(o_{-j}, o_j, \mathbf{a}) \cdot d_\mu^\pi(o_{-j} | o_j), \forall \mathbf{a}]. \quad (5)$$

where o_{-j} are the observations of all other agents and $\tilde{Q}^*(o_{-j}, o_j)$ is a vector of action-values weighted by marginalized visitation probabilities $d_\mu^\pi(o_i | o_j)$ and corresponding to different actions. To this end, we let $\epsilon(o_j) = D_{\cos}(\bar{Q}^*(o_j), \bar{H}(m))$ be the cosine-distance between vectors $\bar{Q}^*(o_j)$ and $\bar{H}(m)$ and consider the **average cosine-distance** ϵ within all clusters, which is defined as:

$$\epsilon \triangleq \sum_m d_\mu^\pi(m) \sum_{o_j \sim m} \bar{d}_m(o_j) \cdot \epsilon(o_j), \quad (6)$$

where $d_\mu^\pi(m)$ is the visitation probability of message m . The result is summarized in Lemma 4.2.

Lemma 4.2. (*Impact of Communication.*) *Consider two optimal policies $\pi_{(j)}^*$ and $\pi_{(j)}$ conditioned on o_j and m_{ij} , respectively, while the observability and policies of all other agents remains the same. The optimal expected average return gap is bounded by:*

$$J(\pi_{(j)}^*) - J(\pi_{(j)}, g) \leq O(\sqrt{\epsilon} Q_{\max}) \quad (7)$$

where Q_{\max} is the maximum action value defined in Eq.(5) and ϵ is the average cosine-distance defined in Eq.(6).

Proof. We give an outline and provide complete proof in Appendix. Since the observability of all other agents $i \neq j$ remains the same, we consider them as a conceptual agent denoted by $-j$. For simplicity, we use π^* to represent $\pi_{(j)}^*$, and π to represent $\pi_{(j)}$ in distribution functions. The proof contains following major steps: (i). Recasting the communication problem as online clustering by rewriting the return gap using Policy Change Lemma 4.1. (ii). Projecting action-value vectors towards cluster centers to quantify the return gap through orthogonal parts related to projection errors. (iii). Deriving an upper bound on the return gap by bounding the orthogonal projection errors using the average cosine-distance within each cluster.

Step 1: Recasting communication problem into online clustering. Viewing the problem as a clustering of o_j , policy $\pi_{(j)}$ (conditioned on m_{ij}) is restricted to taking the same actions for all o_j in the same cluster and under the same message m_{ij} (the clustering label). We rewrite the optimal expected average return gap in Lemma 4.1 in vector form in terms of action-value vectors $\bar{Q}^*(o_j)$ defined in Eq. 5 (with respect to $\pi_{(j)}^*$) and a maximization function $\Phi_{\max}(\bar{Q}^*(o_j)) = \sum_{o_{-j}} \Phi_{\max}(\tilde{Q}^*(o_{-j}, o_j))$ defined as the optimal expected average return conditioned on o_j . These allows us to apply Lemma 4.1

to $J(\pi_{(j)}^*)$ and $J(\pi_{(j)}, g)$ in vector form and rewrite it to obtain:

$$J(\pi_{(j)}^*) - J(\pi_{(j)}, g) \leq \sum_m d_\mu^\pi(m) \left[\sum_{o_j \sim m} \bar{d}_m(o_j) \cdot \Phi_{\max}(\bar{Q}^*(o_j)) - \Phi_{\max} \left(\sum_{o_j \sim m} \bar{d}_m(o_j) \cdot \bar{Q}^*(o_j) \right) \right], \quad (8)$$

where $\bar{d}_m(o_j) = d_\mu^\pi(o_j)/d_\mu^\pi(m)$ is the marginalized probability of o_j in cluster m and $d_\mu^\pi(m)$ is the visitation probability of message m . Then we used the fact that while $J(\pi_{(j)}^*)$ conditioning on complete o_j can achieve maximum for each vector $\bar{Q}^*(o_j)$, policy $\pi_{(j)}$ is conditioned on messages m_{ij} rather than complete o_j and thus must take the same actions for all o_j in the same cluster. Hence we can construct a (potentially sub-optimal) policy to achieve $\Phi_{\max}(\sum_{o_j \sim m} \bar{d}_m(o_j) \cdot \bar{Q}^*(o_j))$, which provides a lower bound on $J(\pi_{(j)}, g)$.

Step 2: Projecting action-value vectors toward cluster centers. To derive a lower bound on $J(\pi_{(j)}, g)$, we construct a policy that conditions on m_{ij} and takes actions based on the action-value vector at the cluster center. We project each action-value vector $\bar{Q}^*(o_j)$ toward its cluster center $\bar{H}(m)$, denoting $Q^\perp(o_j)$ and $\cos \theta_{o_j} \cdot \bar{H}_m$ as the orthogonal and projected parts respectively. It is easy to see that since $\bar{Q}^*(o_j) = Q^\perp(o_j) + \cos \theta_{o_j} \cdot \bar{H}_m$, we have:

$$\Phi_{\max}(\bar{Q}^*(o_j)) \leq \Phi_{\max}(\cos \theta_{o_j} \cdot \bar{H}_m) + \Phi_{\max}(Q^\perp(o_j)). \quad (9)$$

Taking a sum over all o_j in the cluster, we have $\sum_{o_j \sim m} \bar{d}_m(o_j) \Phi_{\max}(\cos \theta_{o_j} \cdot \bar{H}_m) = \Phi_{\max}(\bar{H}_m)$, since the projected components should add up to exactly \bar{H}_m . To bound the return gap obtained in Eq.(8), it remains to bound the orthogonal components relating to the projection error.

Step 3: Deriving the upper bound w.r.t. cosine-distance. This gives us an upper bound on the return gap $J(\pi_{(j)}^*) - J(\pi_{(j)}, g)$, which depends on the orthogonal projection errors and can be further bounded using the average cosine-distance of each cluster. Cosine-distance allows us to encode observations into the same cluster whose corresponding action-values are likely maximized at the same actions. Let $\|\cdot\|_2$ be the L_2 norm. Since the maximum function $\Phi_{\max}(Q^\perp(o_j))$ can be bounded by its L_2 norm $C \cdot \|Q^\perp(o_j)\|_2$ for some constant C , we define a constant Q_{\max} as the maximum absolute action value. We can bound the orthogonal projection errors using cosine-distance: $\Phi_{\max}(Q^\perp(o_j)) \leq O(\sqrt{\epsilon(o_j)} Q_{\max})$. Using the concavity of square root together with Eq.(6), i.e., $\sum_m d_\mu^\pi(m) [\sum_{o_j \sim m} \bar{d}_m(o_j) \cdot \sqrt{\epsilon(o_j)}] \leq \sqrt{\epsilon}$, we derive the desired upper bound. \square

Theorem 4.3. *In n -agent Dec-POMDP, the return gap between policy π^* with full-observability and communication-enabled policy π with partial-observability is bounded by:*

$$J(\pi^*) - J(\pi, g) \leq O(\sqrt{\epsilon n} Q_{\max}). \quad (10)$$

Proof. Beginning from $\pi^* = [\pi_i^*(a_i | o_1, o_2, \dots, o_n), \forall i]$, we can construct a sequence of n policies, each replacing the conditioning on o_j by messages m_{ij} , for $j = 1$ to $j = n$. This will result in policy π with partial observability. Applying Lemma 4.2 n times, we prove the upper bound between $J(\pi^*)$ and $J(\pi, g)$ in this theorem. \square

Remark 4.4. Thm. 4.3 holds for any arbitrary finite number of message labels $|M|$. Furthermore, increasing $|M|$ reduces the average cosine distance (since more clusters are formed) and, consequently, a reduction in the return gap due to the upper bound derived in Thm. 4.3.

An illustrative example. We consider a two-agent matrix game with pay-off Q^* shown in Fig 1. Assume that different observations are equally likely and that agent 2 has a single action in each state. It is easy to see that under an ideal optimal policy $\pi^* = [\pi_1^*, \pi_2^*]$ with full observability (o_1, o_2) can achieve an optimal average reward of $J(\pi_1^*) = 1/2 \cdot [(53.2 + 4.5 + 64.0 + 16.1)/4 + (31.8 + 28.0 + 34.1 + 81.5)/4] = 39.1375$ by choosing the optimal actions in each (o_1, o_2) , i.e., $\pi^* = \operatorname{argmax}_{a_1, a_2} Q^*(o_1, o_2, a_1, a_2)$. Consider a POMDP scenario where agent 1 has only local observation o_1 , and agent 2 can send a 1-bit message $m_{12} = g(o_2)$ encoding its local observation o_2 . Since the message is only 1-bit but there are 4 possible observations

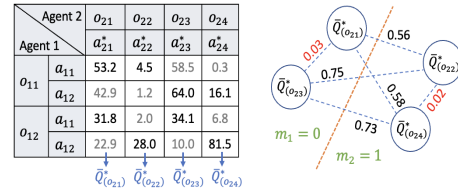


Figure 1: An illustrative example of optimizing message generation m_{12} via clustering to minimize the return gap

o_2 , multiple observations must be encoded into the same message. Thus, agent 1 is restricted to a limited policy class $\pi_1(a_1|o_1, m_{12})$ taking the same actions (or action distributions) under the same o_1 and for all o_2 corresponding to the same message m_{12} . Thm. 4.3 shows that to minimize the return gap between $\pi_1(a_1|o_1, m_{12})$ with partial observation and the ideal optimal policy $\pi^* = [\pi_1^*, \pi_2^*]$ with full observability, we can leverage a message generation function to minimize the average cosine distance ϵ between action values for different observations o_2 . In particular, let $\bar{Q}^*(o_2)$ be a column of Q^* corresponding to o_2 , if $\bar{Q}^*(o_{2i})$ and $\bar{Q}^*(o_{2j})$ are likely maximized at the same actions a_1 , then encoding o_{2i} and o_{2j} to the same message would result in little return gap as formalized in Thm. 4.3. The message generation could be viewed as a clustering problem over o_2 under vector cosine-distance [47]. The left figure in Fig 1 displays the cosine distances calculated between every pair of action value vectors in $\bar{Q}^*(o_{2i})$ and $\bar{Q}^*(o_{2j})$ (which are readily available during centralized training). According to the Thm. 4.3, assigning the same message labels to observations o_2 whose optimal action value vectors have smaller cosine distances would result in smaller return gaps. Hence, we assign message label ‘0’ to $\bar{Q}^*(o_{21})$ and $\bar{Q}^*(o_{23})$, whose cosine distance is 0.03, and message label ‘1’ to $\bar{Q}^*(o_{22})$ and $\bar{Q}^*(o_{24})$, whose cosine distance is 0.02. Accordingly, the message generation in Fig 1 leads to an average return of $J(\pi, g) = 38.775$ with an optimal return gap of $J(\pi^*) - J(\pi, g) = 0.3625$.

4.2 Communication Framework Minimizing the Upper Bound of Average Cosine Distance ϵ

Based on Thm. 4.3, we propose the *Return-Gap-Minimization Communication (RGMComm)* algorithm shown in Fig.(2), which learns the optimal action-value function by performing online clustering to minimize ϵ . It generates communication message labels using joint action-values obtained during centralized training, making it compatible with existing MARL algorithms using the CTDE paradigm. This method is easily implementable as joint action-value functions are readily available in most MARL algorithms like MADDPG [5], QMIX [20], FOP [34], and DOP [22]. Communication can be trained alongside agent policies by efficiently sampling action-values from the replay buffer, allowing its application to continuous state-space problems.

MARL training. We can leverage state-of-the-art MARL algorithms adopting CTDE framework to train agent policies and obtain an estimate of the joint action-value function. Note that we drop time t in the following notations for simplicity. Let $\hat{Q}_\omega(\mathbf{o}, \mathbf{a})$ be a DNN parameterized by ω . We update the parameter ω using an experience replay buffer \mathcal{R} containing tuples $(\mathbf{o}, \mathbf{a}, R, \mathbf{o}')$ and recording the experiences of all agents. The joint action-value function $\hat{Q}_\omega(\mathbf{o}, \mathbf{a})$ is updated as:

$$\mathcal{L}(\omega) = E_{(\mathbf{o}, \mathbf{a}, R, \mathbf{o}')}[(\hat{Q}_\omega(\mathbf{o}, \mathbf{a}) - y)^2], y = R + \gamma \hat{Q}_\omega(\mathbf{o}', \mathbf{a}')|_{\mathbf{a}'} = \pi'(\mathbf{o}'). \quad (11)$$

We note that decisions above may be taken with respect to decentralized policies $\pi = [\pi_i(a_i|o_i, m_{-i}), \forall i]$ in CTDE. Suppose that agents’ policies are parameterized by $\{\theta_1, \dots, \theta_n\}$, respectively. We can update the policies using policy gradient:

$$\nabla_{\theta_i} J(\theta_i) = E_{\mathbf{o}, \mathbf{a} \sim \mathcal{R}} \left[\nabla_{\theta_i} \log \pi_{\theta_i}(a_i|o_i, m_{-i}) \hat{Q}_\omega^{\pi_{\theta_i}}(\mathbf{o}, \mathbf{a}) \right]. \quad (12)$$

Learning message generation We train message generation functions by sampling the action value function and transitions in the replay buffer. It also makes our framework applicable to continuous state-space problems by sampling. Let the message generation functions $g = \{g_1, \dots, g_n\}$ be parameterized by $\xi = \{\xi_1, \dots, \xi_n\}$, respectively. For each agent i , we first sample a random minibatch of K_1 samples $\mathcal{S} = (\mathbf{o}^j, \mathbf{a}^j, R^j, \mathbf{o}^j)$ from the replay buffer \mathcal{R} . Then we sample a set $\mathcal{X}_{-i} = (\mathbf{o}_{-i}, \mathbf{a}_{-i})$ from \mathcal{S} that are top K_2 frequent observation-action pairs. We form the sampled trajectories by combining (o_i, a_i) in \mathcal{S} and in \mathcal{X}_{-i} as $\mathcal{D} = (\mathbf{o}^p, \mathbf{a}^p, R^p, \mathbf{o}^p)$. For obtain the joint action-values, we query the action-value neural networks to get the $\hat{Q}_\omega(o_i, \mathbf{o}_{-i}, a_i, \mathbf{a}_{-i})$ and store the outcome into a set of vectors $\bar{Q}^*(o_i)$ as defined in Eq.(5). We train communication function g_{ξ_i}

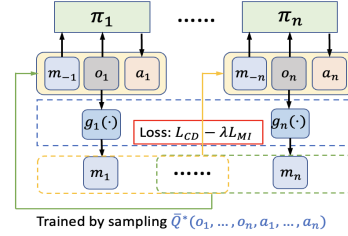


Figure 2: RGMComm Training

with a Regularized Information Maximization(RIM) loss function [13] on the set of vectors:

$$\mathcal{L}(g_{\xi_i}) = L_{CD} - \lambda L_{MI},$$

$$L_{CD} = \sum_{p=1}^{K_1} \sum_{q \in N_j(p)} [D_{cos}(\bar{Q}^*(o_i^p), \bar{Q}^*(o_i^q)) \|m_i^p - m_i^q\|^2], \quad L_{MI} = \sum_{p=1}^{K_1} I(o_i^p; m_i^p), \quad (13)$$

where $m_i = g_{\xi_i}(o_i)$ is optimized by updating parameters ξ_i . The above RIM loss function contains two parts: the first part is a clustering loss L_{CD} that is in the form of Locality-preserving loss [48] – it preserves the locality of the clusters by pushing nearby data points of action-value vectors together. Here $N_j(p)$ is the set of j nearest neighbors $\bar{Q}^*(o_i^p)$, D_{cos} is the cosine-distance between the points $\bar{Q}^*(o_i^p)$ and its neighbor $\bar{Q}^*(o_i^q)$. The second part is a mutual information loss L_{MI} which quantifies the statistical dependency [13] between observation o_i^p and generated clustering labels $m_i^p = g_{\xi_i}(o_i)$. A hyper-parameter $\lambda \in \mathbf{R}$ trades off the two terms. Before calculating the cosine-distance, action-value vectors are normalized and went through the activation function $f((\bar{Q}^*(o_i^p) - \alpha)/\beta)$ for a better clustering result. The complete pseudo-code for training RGMComm is in Appendix.

5 Evaluations

We conduct experiments on POMDP problems with continuous state space (e.g., Multi-Agent Particle Environment [5, 16]). We compare the proposed *Return-Gap-Minimization Communication (RGMComm)* algorithm with state-of-the-art communication-enabled MARL algorithms including *CommNet*[7], *MADDPG*[5] with *partial observability*, *IC3Net* [23], *TarMAC*[9], and *SARNet* [10]. RGMComm significantly outperforms these baselines in all scenarios and achieves nearly-optimal return compared to an ideal MADDPG algorithm with full observability. We also provide an ablation study and illustrate message interpretations using a grid-world maze. We use MADDPG to obtain an estimated action value function and the hyperparameters during training are listed in Appendix.

5.1 Predator-Prey

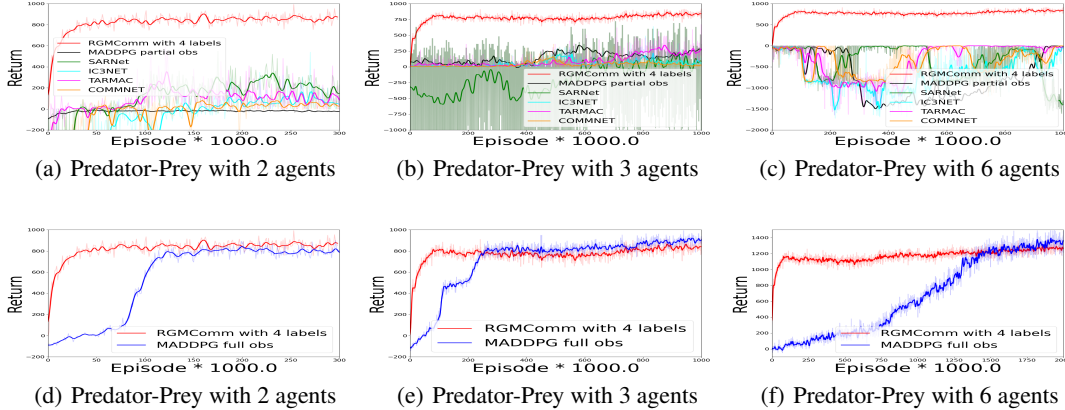


Figure 3: Evaluation on n -agent Predator-Prey tasks: (a)-(c) Comparing RGMComm with baselines with communication: RGMComm converges to a higher mean episode reward than all the baselines. (d)-(f) Comparing RGMComm with full-observability policy: RGMComm achieves nearly optimal mean episode reward in all scenarios with varying numbers of agents, which illustrates its ability to minimize the return gap.

In the Predator-Prey scenario, predators are trained to collaborate to surround and seize prey, while prey are moving randomly. We trained RGMComm with different alphabet size $|M|$ and $N = 2, 3, 6$ agents. Figures 3(a) to 3(c) show that RGMComm outperforms all baselines in Predator-Prey scenarios with 2, 3, and 6 cooperative predators. The figures display learning curves of 300,000, 1,000,000, and 2,000,000 episodes in terms of mean episode reward, averaged over all evaluating episodes (10 episodes evaluated every 1000 episodes). Figures 3(d) to 3(f) show the learning curves of average returns under our RGMComm policy compared with an ideal full-observability policy π^* . We observe that RGMComm achieves near-optimal mean episode reward in all scenarios with varying numbers of agents, which demonstrates its ability to minimize the return gap. The proposed RGMComm algorithm sometimes even converges to a higher mean episode reward since the message

generation function learned from the centralized critic provides a succinct, discrete representation of the optimal action-value structure, leading to less noisy communication signals and allowing agents to discover more efficient decision-making policies conditioned on the message labels. Additionally, the message generation training process uses an online clustering algorithm that does not require a large volume of data, leading to faster convergence, which enables the algorithm to scale well as the number of agents increases.

Fig 4 shows how the total number of message labels affects RGMComm’s performance. We compare the normalized mean episode reward achieved by RGMComm with different numbers of message labels, i.e., $|M| = 0, 2, 4, 8, 16, 32$, normalized by the mean reward achieved by an ideal policy with full-observability (trained using MADDPG). As expected, the mean episode reward increases with the total number of message labels. Remarkably, with only $|M| = 2$ message labels (i.e., 1-bit communication), RGMComm achieves nearly optimal mean episode reward. With more than $|M| = 4$ message labels, RGMComm obtains a higher reward than the policy with full observability, demonstrating that discrete communication allows more efficient policies to be learned in POMDP.

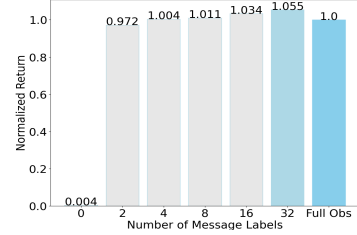
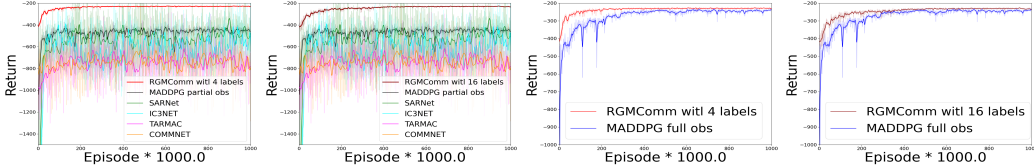


Figure 4: The normalized mean episode reward increases as the total number of message labels increases (Predator-Prey).

5.2 Cooperative Navigation



(a) 4 labels with baselines (b) 16 labels with baselines (c) 4 labels with full obs (d) 16 labels with full obs

Figure 5: Comparisons on Cooperation Navigation tasks: (a)-(b) RGMComm using 4 and 16 message labels (red and dark red lines) both have higher convergence values than all baselines with communication. (c)-(d) RGMComm using 4 or 16 message labels (red and dark red lines) leads to an almost zero return gap and achieves nearly-optimal returns.

In the Cooperative Navigation scenario, we train RGMComm using 4 and 16 message labels. Each agent could observe the nearest landmark with relative positions and velocities without knowing the others’ information. At each timestep, the reward of an agent is given by the distance between the agent and its nearest landmark. A penalty of -1 will be added if a collision occurs between agents. Fig 5(a) and Fig 5(b) show the learning curve in terms of mean episode reward for RGMComm using 4 and 16 message labels compared with baselines with communication. We can see that RGMComm converges to a much higher reward than all the baselines at a faster convergence speed. Fig 5(c) and Fig 5(d) show that RGMComm using 4 or 16 message labels leads to almost zero return gap and achieves nearly-optimal returns in both cases. Fig 6 plots the average cosine-distance and the corresponding return gap (between RGMComm and full-observability policy) using 4, 6, 8 message labels. The cosine-distance ϵ is averaged over different clusters and different vectors $\bar{Q}^*(o_j)$ in each cluster. We note that the Q_{\max} for 4-, 6-, 8-label RGMComm policy is 721, 739, 754 respectively. To calculate the return gap, we evaluate RGMComm and full-observation policy with respect to the mean episode rewards by taking the average over the last 30 episodes after each algorithm converged. The numerical results justify our analysis in Thm. 4.3 as return gaps are indeed bounded by

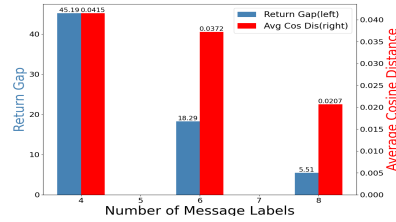
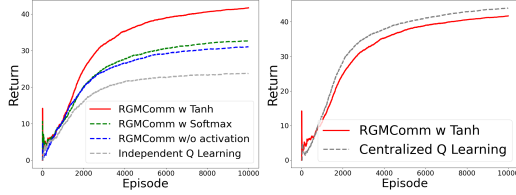


Figure 6: The return gap(left) is bounded by average cosine-distance(right) and diminishes as average cosine-distance(right) decreases due to the use of more message labels.

$O(\sqrt{\epsilon n Q_{\max}})$, the average return gap diminishes as the average cosine-distance decreases due to the use of more message labels.

5.3 Ablation Study

We further provide an ablation study on the clustering algorithm by choosing different activation functions for normalizing action value vectors $\bar{Q}^*(o_j)$, which effectively leads to different distance metrics in clustering. We compare the achieved average returns by using Softmax function, hyperbolic tangent (Tanh) function, and not using any activation functions in our proposed RGMComm algorithm with two baselines - independent Q learning and centralized Q learning algorithms (by allowing π^* to have full-observability). Fig 7(a) shows RGMComm with Tanh can converge to a higher return, compared to RGMComm with no activation function, RGMComm with Softmax, and Independent Q learning algorithm. Fig 7(b) shows RGMComm with Tanh and cosine-distance can achieve a nearly-optimal return compared to centralized Q learning full observability algorithm. This is because such S-shape functions can push larger action-values toward 1, which helps the online clustering algorithm under cosine-distance to group the action-values that are likely maximized at the same actions.



(a) RGMComm w base-(b) RGMComm w full obs lines

Figure 7: RGMComm with Tanh(red) outperforms all baselines with partial observation(shown is Fig (a)) and converges to almost the optimal mean episode reward achieved by centralized Q learning with full observation(shown in Fig (b)).

5.4 Communication Message Interpretations

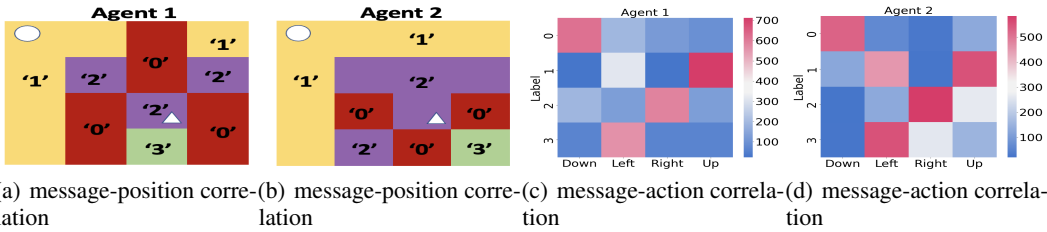


Figure 8: (a)-(b): agents are more likely to send label ‘1’ when closer to higher-reward target(circle); while more likely to send label ‘2’ when closer to lower-reward target(triangle); (c)-(d): both agents are more likely to take action ‘down’, ‘up’, ‘right’, ‘left’ conditioned receiving label ‘0’, ‘1’, ‘2’, and ‘3’, respectively.

The discrete message labels used in RGMComm are easily interpretable. Considering a grid-world maze environment for visual clarity. The relationship between message labels, local observations, and agent actions is investigated in 8(a) and 8(b), visualizing the frequency of message labels emitted by agents in different positions during training. Agents tend to send specific labels (we use ‘red’, ‘yellow’, ‘purple’, and ‘green’ to represent the positions where agents have higher probabilities to send message labels ‘0’, ‘1’, ‘2’, and ‘3’, respectively.) depending on their proximity to high-reward(circle) or low-reward(triangle) targets. The correlation between actions and received messages is also visualized for two agents in 8(c) and 8(d). These visualizations illustrate that agents are more likely to take certain actions based on the received labels, allowing for effective coordination. For instance, we can see that when an RGMComm agent approaches the high-reward target, it will utter a label ‘1’, instructing other agents to move ‘up’ or ‘left’, which effectively guides other agents to approach the same target located at the upper left corner of the map. In summary, RGMComm enables interpretable discrete communication paving the path for task-specific interpretations during training.

6 Conclusion

This paper proposes a discrete communication framework for MARL using a finite-size discrete alphabet and an online clustering approach for message generation. It quantifies the optimal return gap

between ideal and communication-enabled policies with a closed-form upper bound. A new MARL communication algorithm is introduced, outperforming existing methods with few-bit messages. Future work will focus on exploring message label structures suitable for human use.

References

- [1] Cao, Y., W. Yu, W. Ren, G. Chen. An overview of recent progress in the study of distributed multi-agent coordination. *IEEE Transactions on Industrial Informatics*, 9(1):427–438, 2013.
- [2] Li, L., A. Martinoli, Y. S. Abu-Mostafa. Emergent specialization in swarm systems. In *Proceedings of the Third International Conference on Intelligent Data Engineering and Automated Learning*, IDEAL '02, page 261–266. Springer-Verlag, Berlin, Heidelberg, 2002.
- [3] Freed, B., R. James, G. Sartoretti, H. Choset. Sparse discrete communication learning for multi-agent cooperation through backpropagation. In *2020 IEEE/RSJ International Conference on Intelligent Robots and Systems (IROS)*, pages 7993–7998. IEEE, 2020.
- [4] Paulos, J., S. W. Chen, D. Shishika, V. Kumar. Decentralization of multiagent policies by learning what to communicate. In *2019 International Conference on Robotics and Automation (ICRA)*, pages 7990–7996. IEEE, 2019.
- [5] Lowe, R., Y. Wu, A. Tamar, J. Harb, P. Abbeel, I. Mordatch. Multi-agent actor-critic for mixed cooperative-competitive environments, 2017.
- [6] Foerster, J. N., Y. M. Assael, N. de Freitas, S. Whiteson. Learning to communicate with deep multi-agent reinforcement learning, 2016.
- [7] Sukhbaatar, S., A. Szlam, R. Fergus. Learning multiagent communication with backpropagation, 2016.
- [8] Jiang, J., Z. Lu. Learning attentional communication for multi-agent cooperation, 2018.
- [9] Das, A., T. Gervet, J. Romoff, D. Batra, D. Parikh, M. Rabbat, J. Pineau. Tarmac: Targeted multi-agent communication, 2018.
- [10] Rangwala, M., R. Williams. Learning multi-agent communication through structured attentive reasoning. In *Proceedings of the 34th International Conference on Neural Information Processing Systems*, NIPS'20. Curran Associates Inc., Red Hook, NY, USA, 2020.
- [11] Krause, A., P. Perona, R. Gomes. Discriminative clustering by regularized information maximization. *Advances in neural information processing systems*, 23, 2010.
- [12] Thomas, M., A. T. Joy. *Elements of information theory*. Wiley-Interscience, 2006.
- [13] Hu, W., T. Miyato, S. Tokui, E. Matsumoto, M. Sugiyama. Learning discrete representations via information maximizing self-augmented training. In *International conference on machine learning*, pages 1558–1567. PMLR, 2017.
- [14] Li, P., H. Tang, T. Yang, et al. Pmic: Improving multi-agent reinforcement learning with progressive mutual information collaboration. *arXiv preprint arXiv:2203.08553*, 2022.
- [15] Brown, T., B. Mann, N. Ryder, et al. Language models are few-shot learners. *Advances in neural information processing systems*, 33:1877–1901, 2020.
- [16] Mordatch, I., P. Abbeel. Emergence of grounded compositional language in multi-agent populations, 2017.
- [17] Freed, B., G. Sartoretti, H. Choset. Simultaneous policy and discrete communication learning for multi-agent cooperation. *IEEE Robotics and Automation Letters*, 5(2):2498–2505, 2020.
- [18] Duan, H., L. Yang, J. Fang, H. Li. Fast inverse-free sparse bayesian learning via relaxed evidence lower bound maximization. *IEEE Signal Processing Letters*, 24(6):774–778, 2017.

- [19] Hoffman, M. D., M. J. Johnson. Elbo surgery: yet another way to carve up the variational evidence lower bound. In *Workshop in Advances in Approximate Bayesian Inference, NIPS*, vol. 1. 2016.
- [20] Rashid, T., M. Samvelyan, C. Schroeder, G. Farquhar, J. Foerster, S. Whiteson. Qmix: Monotonic value function factorisation for deep multi-agent reinforcement learning. In *International conference on machine learning*, pages 4295–4304. PMLR, 2018.
- [21] Zhou, H., T. Lan, V. Aggarwal. Pac: Assisted value factorization with counterfactual predictions in multi-agent reinforcement learning. *Advances in Neural Information Processing Systems*, 35:15757–15769, 2022.
- [22] Wang, Y., B. Han, T. Wang, H. Dong, C. Zhang. Dop: Off-policy multi-agent decomposed policy gradients. In *International Conference on Learning Representations*. 2020.
- [23] Singh, A., T. Jain, S. Sukhbaatar. Learning when to communicate at scale in multiagent cooperative and competitive tasks, 2018.
- [24] Busoniu, L., R. Babuska, B. De Schutter. A comprehensive survey of multiagent reinforcement learning. *IEEE Transactions on Systems, Man, and Cybernetics, Part C (Applications and Reviews)*, 38(2):156–172, 2008.
- [25] Zhou, H., T. Lan, V. Aggarwal. Value functions factorization with latent state information sharing in decentralized multi-agent policy gradients. *IEEE Transactions on Emerging Topics in Computational Intelligence*, 2023.
- [26] Gogineni, K., Y. Mei, P. Wei, T. Lan, G. Venkataramani. Accmer: Accelerating multi-agent experience replay with cache locality-aware prioritization. *arXiv preprint arXiv:2306.00187*, 2023.
- [27] Bernstein, D. S., R. Givan, N. Immerman, S. Zilberstein. The complexity of decentralized control of markov decision processes. *Mathematics of operations research*, 27(4):819–840, 2002.
- [28] Foerster, J., G. Farquhar, T. Afouras, N. Nardelli, S. Whiteson. Counterfactual multi-agent policy gradients. In *Proceedings of the AAAI conference on artificial intelligence*, vol. 32. 2018.
- [29] Iqbal, S., F. Sha. Actor-attention-critic for multi-agent reinforcement learning. In *International conference on machine learning*, pages 2961–2970. PMLR, 2019.
- [30] Sunehag, P., G. Lever, A. Gruslys, et al. Value-decomposition networks for cooperative multi-agent learning. *arXiv preprint arXiv:1706.05296*, 2017.
- [31] Pesce, E., G. Montana. Improving coordination in small-scale multi-agent deep reinforcement learning through memory-driven communication. *Machine Learning*, 109(9-10):1727–1747, 2020.
- [32] Charlot, P., C. Jacobs, D. Gordon, et al. The third realization of the international celestial reference frame by very long baseline interferometry. *Astronomy & Astrophysics*, 644:A159, 2020.
- [33] Yu, C., A. Velu, E. Vinitsky, Y. Wang, A. Bayen, Y. Wu. The surprising effectiveness of ppo in cooperative, multi-agent games. *arXiv preprint arXiv:2103.01955*, 2021.
- [34] Zhang, T., Y. Li, C. Wang, G. Xie, Z. Lu. Fop: Factorizing optimal joint policy of maximum-entropy multi-agent reinforcement learning. In *International Conference on Machine Learning*, pages 12491–12500. PMLR, 2021.
- [35] Peng, P., Y. Wen, Y. Yang, Q. Yuan, Z. Tang, H. Long, J. Wang. Multiagent bidirectionally-coordinated nets: Emergence of human-level coordination in learning to play starcraft combat games. *arXiv preprint arXiv:1703.10069*, 2017.
- [36] Mao, H., Z. Zhang, Z. Xiao, Z. Gong, Y. Ni. Learning agent communication under limited bandwidth by message pruning, 2019.

- [37] Li, S., J. K. Gupta, P. Morales, R. Allen, M. J. Kochenderfer. Deep implicit coordination graphs for multi-agent reinforcement learning, 2020.
- [38] Ding, Z., T. Huang, Z. Lu. Learning individually inferred communication for multi-agent cooperation. *Advances in Neural Information Processing Systems*, 33:22069–22079, 2020.
- [39] Sheng, J., X. Wang, B. Jin, J. Yan, W. Li, T.-H. Chang, J. Wang, H. Zha. Learning structured communication for multi-agent reinforcement learning. *Autonomous Agents and Multi-Agent Systems*, 36(2):1–31, 2022.
- [40] LeCun, Y., Y. Bengio, G. Hinton. Deep learning. *nature*, 521(7553):436–444, 2015.
- [41] Tucker, M., H. Li, S. Agrawal, D. Hughes, K. Sycara, M. Lewis, J. A. Shah. Emergent discrete communication in semantic spaces. *Advances in Neural Information Processing Systems*, 34:10574–10586, 2021.
- [42] Liu, D., A. M. Lamb, K. Kawaguchi, A. G. ALIAS PARTH GOYAL, C. Sun, M. C. Mozer, Y. Bengio. Discrete-valued neural communication. *Advances in Neural Information Processing Systems*, 34:2109–2121, 2021.
- [43] Li, S., Y. Zhou, R. Allen, M. J. Kochenderfer. Learning emergent discrete message communication for cooperative reinforcement learning. In *2022 International Conference on Robotics and Automation (ICRA)*, pages 5511–5517. IEEE, 2022.
- [44] Su, K., Z. Lu. Divergence-regularized multi-agent actor-critic. In *International Conference on Machine Learning*, pages 20580–20603. PMLR, 2022.
- [45] Mei, Y., H. Zhou, T. Lan. Remix: Regret minimization for monotonic value function factorization in multiagent reinforcement learning. *arXiv preprint arXiv:2302.05593*, 2023.
- [46] Mei, Y., H. Zhou, T. Lan, G. Venkataramani, P. Wei. Mac-po: Multi-agent experience replay via collective priority optimization. In *Proceedings of the 2023 International Conference on Autonomous Agents and Multiagent Systems, AAMAS '23*, page 466–475. International Foundation for Autonomous Agents and Multiagent Systems, 2023.
- [47] Muflikhah, L., B. Baharudin. Document clustering using concept space and cosine similarity measurement. In *2009 International Conference on Computer Technology and Development*, vol. 1, pages 58–62. IEEE, 2009.
- [48] Huang, P., Y. Huang, W. Wang, L. Wang. Deep embedding network for clustering. In *2014 22nd International Conference on Pattern Recognition*, pages 1532–1537. 2014.
- [49] Sutton, R. S., A. G. Barto. *Reinforcement learning: An introduction*. MIT press, 2018.
- [50] Son, K., D. Kim, W. J. Kang, D. E. Hostallero, Y. Yi. Qtran: Learning to factorize with transformation for cooperative multi-agent reinforcement learning. In *International conference on machine learning*, pages 5887–5896. PMLR, 2019.
- [51] Yang, Y., J. Hao, B. Liao, K. Shao, G. Chen, W. Liu, H. Tang. Qatten: A general framework for cooperative multiagent reinforcement learning. *arXiv preprint arXiv:2002.03939*, 2020.
- [52] Peng, B., T. Rashid, C. Schroeder de Witt, P.-A. Kamienny, P. Torr, W. Böhmer, S. Whiteson. Facmac: Factored multi-agent centralised policy gradients. *Advances in Neural Information Processing Systems*, 34:12208–12221, 2021.
- [53] Vaswani, A., N. Shazeer, N. Parmar, J. Uszkoreit, L. Jones, A. N. Gomez, L. Kaiser, I. Polosukhin. Attention is all you need, 2017.
- [54] Niu, Y., R. R. Paleja, M. C. Gombolay. Multi-agent graph-attention communication and teaming. In *AAMAS*, pages 964–973. 2021.

A Detailed Discussion about Related Work

Multi-Agent Reinforcement Learning (MARL): MARL [24] has gained significant attention in the field of Reinforcement Learning (RL). This paper focuses on cooperative MARL, which is typically modeled as a Decentralized Partially Observable Markov Decision Process (Dec-POMDP)[27], where all agents aim to maximize the long-term return by sharing a reward. The Centralized Training with Decentralized Execution (CTDE) paradigm[5] is widely used in cooperative MARL. This approach employs a centralized value function for training and decentralized policies for scalability. During training, agents use centralized information to learn by pooling observations and actions of all agents in a critic network. The critic then provides feedback in the form of a joint action-value function. However, during execution, each agent only has access to its own observation and communication messages. Many MARL algorithms, including COMA [28], MAAC [29], VDN [30], QMIX [20], MD-MADDPG [31], FAC-MADDPG [32], MA-PPO [33], DOP [22], FOP [34], and PMIC [14], adopt CTDE paradigms to improve performance in cooperative MARL.

COMA [28] proposes a counterfactual baseline to address multi-agent credit assignment in cooperative settings. MAAC [29] employs a self-attention mechanism to integrate local observation and action of each agent, providing structured information to the centralized critic. Value decomposition [49, 20, 50–52] is a popular class of cooperative MARL algorithms that express the global Q-function as a function of individual Q-functions, satisfying Individual-Global-Max (IGM) which ensures optimal actions of individual Q-functions correspond to the optimal joint action of the global Q-function. QMIX [20] is a representative of value decomposition methods that uses a hypernet to enforce the monotonicity of the global Q-function in terms of individual Q-functions, a sufficient condition for IGM. DOP [22] combines value decomposition with policy gradient, using a linear value decomposition that also satisfies IGM. FOP [34] combines value decomposition with entropy regularization, using a more general condition, Individual-Global-Optimal, to replace IGM. This paper proposes a decentralized communication framework for MARL using a clustering algorithm over the optimal action-value function for different local observations at each agent, where the clustering labels are the messages to be shared. Our clustering targets joint action values that are available in most state-of-the-art MARL algorithms adopting CTDE mentioned before. Our proposed solution can be easily integrated into these algorithms by sampling the joint action values. The resulting algorithm generates naturally interpretable discrete messages and easily extends to MARL problems with continuous state space by sampling the replay buffer.

MARL with Communication: Communication allows agents to share information so that they can perform tasks cooperatively. Learning communication in MARL has been greatly advanced recently. CommNet[7], a recurrent communication model, averages the hidden states for centralized communication, which however inevitably leads to information loss. BiCNet [35] trains a bi-directional communication channel using recurrent neural networks to integrate messages from all the agents. Both CommNet and BiCNet use a communication channel where each agent sends continuous messages to and receives from all other agents. In such a case, there is no doubt that agents can be flooded by information as the number of agents grows and cost lots of energy. IC3Net [23] and Gated-ACML [36] both propose the gating mechanism to adaptive judge whether the agent needs to send messages to others according to its current state. Instead of centralized aggregation and averaging, TarMAC[9] uses multi-headed attention to distribute information to other agents. Basically, TarMAC is still a traditional broadcast approach (all-to-all communication) with the attention that allows agents to turn a blind eye to received inconsequential and continuous messages. ATOC[8] uses a bidirectional recurrent network as a communication channel which can be seen as a more complex gate mechanism to decide when to speak to predefined neighboring agents. DICG[37] uses graph convolution to implicitly pass information between agents. While SARNet [10] extends the structure of both MD-MADDPG[31] and TarMAC[9] by working with independent memory states and computing the relevance of communicated information through query-key pairs of soft-attention[53]. In [38], I2C proposes that each agent only communicates with those who are in its observation range and affect its decisions. [54] propose a graph-attention communication protocol to help with the problems of when to communicate and whom to address messages to. LSC[39] adopts an auxiliary task to learn hierarchical communication structures.

However, these works generated communication messages using Deep Neural Networks(DNN) which are considered as large black-boxes whose superior performance comes at the cost of using millions or even billions of parameters [15, 40] making the communication messages hard to explain. In addition,

the previous communication protocols assumed agents can exchange continuous real-valued messages containing a potentially unbounded quantity of information. In reality, communication networks typically support discrete (e.g., digital) communication, and have limits on rates of information transfer. Such a communication network may become overburdened if all agents communicate maximally with each other using continuous messages.

There are also some works assume that agents can send discrete messages to all agents within reach of communication [6, 5, 16, 17, 3, 41–43], but none of above works proves the policy regret minimization which means there is no performance guarantee and they are only heuristic designs.

B Background Knowledge

B.1 Centralized Training and Decentralized Execution (CTDE)

Our method employs the Centralized Training Decentralized Execution Actor-Critic Framework for reinforcement learning, which trains agents using centralized information (pooling observations and actions of multiple agents in a critic network) but executes them in a decentralized manner online (allowing each policy network to access only local observation). This framework consists of two components: an actor and a critic. Each agent’s actor takes actions based on its local observation of the environment, while the centralized critic has access to all local observations and actions during training and provides feedback in the form of a joint action-value function. However, during execution, each agent only has access to its own observation and communication messages.

Due to the constraints imposed by the page limit, we are unable to provide detailed information on previous works. However, in Section 2, we have referenced several previous works that introduce the CTDE paradigm. For instance, the MADDPG algorithm, proposed in [5], provides an elaborate description of the paradigm. We will further clarify this in the revised version.

B.2 Observation Action History τ_i :

In a Partially Observable Markov Decision Process (POMDP), the agent lacks complete information about the current state of the environment and, as a result, often maintains a belief state that reflects its current uncertainty regarding the state. One way to represent this belief state is by utilizing the history of observations and actions. This approach can be particularly valuable in situations where the environment is highly stochastic, and there is significant ambiguity regarding the current state if only the most recent observations are considered. This is a standard method employed in many POMDP works such as [44] referenced in our paper. We wanted to point this out and state that our results remain the same if observations are replaced by the history of observations and actions as necessitated by POMDP.

C Proofs

C.1 Proofs for Lemma 4.1

Proof. We prove the result in this lemma by leveraging observation-based state value function $V^\pi(o)$ in Eq.(2) and the corresponding action value function $Q^\pi(o, a) = \mathbb{E}_\pi \left[\sum_{i=0}^{\infty} \gamma^i \cdot R_{t+i} \mid o_t = o, a_t = a \right]$ to unroll the Dec-POMDP. Here we consider all other agents $i \neq j$ as a conceptual agent denoted by $-j$.

$$\begin{aligned}
& J(\pi^*) - J(\pi, g) \\
&= E_\mu(1 - \gamma)[V^*(\mathbf{o}(0)) - V^\pi(\mathbf{o}(0))], \\
&= E_\mu(1 - \gamma)[V^*(o_{-j}(0), o_j(0)) - V^\pi(o_{-j}(0), o_j(0))], \\
&= E_\mu(1 - \gamma)[V^*(o_{-j}(0), o_j(0)) - Q^*(o_{-j}(0), o_j(0), \mathbf{a}_0^\pi) + Q^*(o_{-j}(0), o_j(0), \mathbf{a}_0^\pi) - Q^\pi(o_{-j}(0), o_j(0), \mathbf{a}_0^\pi)], \\
&= E_\mu(1 - \gamma)[\Delta^\pi(o_{-j}(0), o_j(0), \mathbf{a}_0^\pi) + (Q^* - Q^\pi)], \\
&= E_\mu(1 - \gamma)[\Delta^\pi(o_{-j}(0), o_j(0), \mathbf{a}_0^\pi) + E_{o_{-j}(1), o_j(1) \sim P(\cdot | o_{-j}(0), o_j(0), \mathbf{a}_0^\pi)}[\gamma(V^*(o_{-j}(1), o_j(1)) - V^\pi(o_{-j}(1), o_j(1)))]], \\
&= E_{\mu, o_{-j}(t), o_j(t) \sim P}(1 - \gamma) \left[\sum_{t=0}^{\infty} \gamma^t \Delta(o_{-j}(t), o_j(t), \mathbf{a}_t^\pi) | \mathbf{a}_t^\pi \right], \\
&= E_{o_{-j}, o_j \sim d_\mu^\pi, \mathbf{a}^\pi = \pi(o_{-j}, g(o_j))} [\Delta(o_{-j}, o_j, \mathbf{a}^\pi) | \mathbf{a}^\pi], \\
&= \sum_m \sum_{o_j \sim m} \sum_{o_{-j}} \Delta(o_{-j}(t), o_j(t), \mathbf{a}_t^\pi) \cdot d_\mu^\pi(o_{-j}, o_j), \\
&= \sum_m \sum_{o_j \sim m} \sum_{o_{-j}} [Q^*(o_{-j}, o_j, \mathbf{a}_t^{\pi^*}) - Q^*(o_{-j}, o_j, \mathbf{a}_t^\pi)] \cdot d_\mu^\pi(o_{-j}, o_j), \\
&\leq \sum_m \sum_{o_j \sim m} \sum_{o_{-j}} [Q^*(o_{-j}, o_j, \mathbf{a}_t^{\pi^*}) - Q(o_{-j}, o_j, \mathbf{a}_t^\pi)] \cdot d_\mu^\pi(o_{-j}, o_j), \\
&\leq \sum_m \sum_{\mathbf{o} \sim m} [Q^*(\mathbf{o}, \mathbf{a}_t^{\pi^*}) - Q^\pi(\mathbf{o}, \mathbf{a}_t^\pi)] \cdot d_\mu^\pi(\mathbf{o}),
\end{aligned} \tag{14}$$

Step 1 is to use Eq.(3) in the main paper with initial observation distribution $\mathbf{o}(0) \sim \mu$ at time $t = 0$ to re-write the average expected return gap; Step 2 is separate the observations as agent j and the other agents as a single conceptual agent $-j$, then $\mathbf{o} = (o_{-j}, o_j)$; Step 3 and step 4 are to obtain the sub-optimality-gap of policy π , defined as $\Delta^\pi(\mathbf{o}, \mathbf{a}) = V^*(\mathbf{o}) - Q^*(\mathbf{o}, \mathbf{a}^\pi) = Q^*(\mathbf{o}, \mathbf{a}^{\pi^*}) - Q^*(\mathbf{o}, \mathbf{a}^\pi)$, by subtracting and plus a action-value function $Q^*(o_{-j}(0), o_j(0), \mathbf{a}_0^\pi)$; Step 5 is to unroll the Markov chain from time $t = 0$ to time $t = 1$; Step 6 is to use sub-optimality-gap accumulated for all time steps to represent the return gap; Step 7 and step 8 is to absorb the discount factor $1 - \gamma$ by multiplying the $d_\mu^\pi(\mathbf{o}) = (1 - \gamma) \sum_{t=0}^{\infty} P(\mathbf{o}_t = \mathbf{o} | \pi, \mu)$ which is the γ -discounted visitation probability of observations \mathbf{o} under policy π given initial observation distribution μ ; Step 9 is to revert $\Delta^\pi(\mathbf{o}, \mathbf{a})$ back to $Q^*(\mathbf{o}, \mathbf{a}^{\pi^*}) - Q^*(\mathbf{o}, \mathbf{a}^\pi)$; Step 10 is to replace the second term $Q^*(\mathbf{o}, \mathbf{a}^\pi)$ with $Q^\pi(\mathbf{o}, \mathbf{a}^\pi)$. Since $Q^*(\mathbf{o}, \mathbf{a}^{\pi^*})$ is larger than $Q^\pi(\mathbf{o}, \mathbf{a}^\pi)$, therefore, the inequality is valid. \square

C.2 Proofs for Lemma 4.2

Proof. Since the observability of all other agents $i \neq j$ remains the same, we consider them as a conceptual agent denoted by $-j$. For simplicity, we use π^* to represent $\pi_{(j)}^*$, and π to represent $\pi_{(j)}$ in distribution functions. Similar to the illustrative example, we define the action value vector corresponding observation o_j , i.e.,

$$\bar{Q}^*(o_j) = [\tilde{Q}^*(o_{-j}, o_j), \forall o_{-j}], \tag{15}$$

where o_{-j} are the observations of all other agents and $\tilde{Q}^*(o_{-j}, o_j)$ is a vector of action values weighted by marginalized visitation probabilities $d_\mu^\pi(o_{-j} | o_j)$ and corresponding to different actions:

$$\tilde{Q}^*(o_{-j}, o_j) = [Q^*(o_{-j}, o_j, \mathbf{a}) \cdot d_\mu^\pi(o_{-j} | o_j), \forall \mathbf{a}], \forall o_{-j} \sim d_\mu^\pi(o_{-j} | o_j), \forall \mathbf{a} \sim \mu^\pi(o_{-j}, o_j, \mathbf{a}). \tag{16}$$

Here $\mu^\pi(\mathbf{o}, \mathbf{a})$ denotes the observation-action distribution given a policy π , which means $\mu^\pi(\mathbf{o}, \mathbf{a}) = d_\mu^\pi(\mathbf{o})\pi(\mathbf{a} | \mathbf{o})$. We also denote $d_\mu^\pi(m)$ is the visitation probability of message m , and $\bar{d}_m(o_j)$ is the marginalized probability of o_j in cluster m , i.e.,

$$d_\mu^\pi(m) = \sum_{o_j \sim m} d_\mu^\pi(o_j), \quad \bar{d}_m(o_j) = \frac{d_\mu^\pi(o_j)}{d_\mu^\pi(m)}, \tag{17}$$

Since the optimal return $J(\pi_{(j)}^*)$ is calculated from the action values by $\max_{\mathbf{a}} Q(\mathbf{o}, \mathbf{a})$, we rewrite this in the vector form by defining a maximization function $\Phi_{\max}(\tilde{Q}^*(o_{-j}, o_j))$ that returns the largest

component of vector $\tilde{Q}^*(o_{-j}, o_j)$. With slight abuse of notations, we also define $\Phi_{\max}(\bar{Q}^*(o_j)) = \sum_{o_{-j}} \Phi_{\max}(\tilde{Q}^*(o_{-j}, o_j))$ as the expected average return conditioned on o_j . Then $\sum_{o_j \sim m} \bar{d}_m(o_j) \cdot \Phi_{\max}(\bar{Q}^*(o_j))$ could be defined as selecting the action from optimal policy $\pi_{(j)}^*$ where agent chooses different action distribution to maximize $(\bar{Q}^*(o_j))$. We could re-write this term with the action-value function as:

$$\begin{aligned}
& \sum_{o_j \sim m} \bar{d}_m(o_j) \cdot \Phi_{\max}(\bar{Q}^*(o_j)) \\
&= \sum_{o_j \sim m} \bar{d}_m(o_j) \cdot \sum_{o_{-j}} \max_{\mathbf{a}} [Q^*(o_{-j}, o_j, \mathbf{a}) \cdot d_{\mu}^{\pi}(o_{-j}|o_j)], \\
&= \sum_{o_j \sim m} \left(\frac{d_{\mu}^{\pi}(o_j)}{d_{\mu}^{\pi}(m)} \right) \cdot \sum_{o_{-j}} \max_{\mathbf{a}} [Q^*(o_{-j}, o_j, \mathbf{a}) \cdot d_{\mu}^{\pi}(o_{-j}|o_j)], \\
&= \left(\frac{1}{d_{\mu}^{\pi}(m)} \right) \sum_{o_j \sim m} d_{\mu}^{\pi}(o_j) \sum_{o_{-j}} \max_{\mathbf{a}} [Q^*(o_{-j}, o_j, \mathbf{a}) d_{\mu}^{\pi}(o_{-j}|o_j)],
\end{aligned} \tag{18}$$

then we used the fact that while $J(\pi_{(j)}^*)$ conditioning on complete o_j can achieve maximum for each vector $\bar{Q}^*(o_j)$, policy $\pi_{(j)}$ is conditioned on messages m_{ij} rather than complete o_j and thus must take the same actions for all o_j in the same cluster. Hence we can construct a (potentially sub-optimal) policy to achieve $\Phi_{\max}(\sum_{o_j \sim m} \bar{d}_m(o_j) \cdot \bar{Q}^*(o_j))$ which provides a lower bound on $J(\pi_{(j)}, g)$. Plugging in Eq.(17), $\Phi_{\max}(\sum_{o_j \sim m} \bar{d}_m(o_j) \cdot \bar{Q}^*(o_j))$ can be re-written as:

$$\begin{aligned}
& \Phi_{\max} \left(\sum_{o_j \sim m} \bar{d}_m(o_j) \cdot \bar{Q}^*(o_j) \right) \\
&= \sum_{o_{-j}} \max_{\mathbf{a}} \left[\sum_{o_j \sim m} \bar{d}_m(o_j) Q^*(o_{-j}, o_j, \mathbf{a}) \cdot d_{\mu}^{\pi}(o_{-j}|o_j) \right], \\
&= \sum_{o_{-j}} \max_{\mathbf{a}} \left[\sum_{o_j \sim m} \left(\frac{d_{\mu}^{\pi}(o_j)}{d_{\mu}^{\pi}(m)} \right) Q^*(o_{-j}, o_j, \mathbf{a}) \cdot d_{\mu}^{\pi}(o_{-j}|o_j) \right],
\end{aligned} \tag{19}$$

Multiplying the two equations above Eq.(19) and Eq.(18) with $d_{\mu}^{\pi}(m)$ which is the visitation probability of message m to replace the term $\sum_{o_j \sim m} \sum_{o_{-j}} [Q^*(o_{-j}, o_j, \mathbf{a}^*) - Q(o_{-j}, o_j, \mathbf{a})] \cdot d_{\mu}^{\pi}(o_{-j}, o_j)$ in the Eq.(14), we obtain an upper bound on the return gap:

$$\begin{aligned}
& J(\pi_{(j)}^*) - J(\pi_{(j)}, g) \\
&\leq \sum_m \sum_{o_j \sim m} \sum_{o_{-j}} [Q^*(o_{-j}, o_j, \mathbf{a}^*) - Q(o_{-j}, o_j, \mathbf{a})] \cdot d_{\mu}^{\pi}(o_{-j}, o_j), \\
&= \sum_m d_{\mu}^{\pi}(m) \left[\sum_{o_j \sim m} \bar{d}_m(o_j) \cdot \Phi_{\max}(\bar{Q}^*(o_j)) \right. \\
&\quad \left. - \Phi_{\max} \left(\sum_{o_j \sim m} \bar{d}_m(o_j) \cdot \bar{Q}^*(o_j) \right) \right].
\end{aligned} \tag{20}$$

To quantify the resulting return gap, we denote the center of a cluster of vectors $\bar{Q}^*(o_j)$ for $o_j \sim m$ under message m as:

$$\bar{H}(m) = \sum_{o_j \sim m} \bar{d}_m(o_j) \cdot \bar{Q}^*(o_j). \tag{21}$$

We contract clustering labels to make corresponding joint action-values $\{\bar{Q}^*(o_j) : g(o_j) = m\}$ close to its center $\bar{H}(m)$. Specifically, the average cosine-distance is bounded by a small ϵ for each message m , i.e.,

$$\begin{aligned}
& \sum_{o_j \sim m} D(\bar{Q}^*(o_j), \bar{H}(m)) \cdot d_{\mu}^{\pi}(m) \\
&\leq \sum_{o_j \sim m} \epsilon(o_j) \cdot d_{\mu}^{\pi}(m) \leq \epsilon, \quad \forall m \in M.
\end{aligned} \tag{22}$$

where $\epsilon(o_j) = \sum_{o_j \sim m} D_{\cos}(\bar{Q}^*(o_j), \bar{H}(m))/K$, K is the number observations with the same label m , and $D_{\cos}(A, B) = 1 - \frac{A \cdot B}{\|A\| \|B\|}$ is the cosine distance function between two vectors A and B .

For each pair of two vectors $\bar{Q}^*(o_j)$ and $\bar{H}(m)$ with $D(\bar{Q}^*(o_j), \bar{H}(m)) \leq \epsilon(o_j)$, we use $\cos \theta_{o_j}$ to denote the cosine-similarity between each $\bar{Q}^*(o_j)$ and its center $\bar{H}(m)$. Then we have the cosine distance $D(\bar{Q}^*(o_j), \bar{H}(m)) = 1 - \cos \theta_{o_j} \leq \epsilon(o_j)$. By projecting $\bar{Q}^*(o_j)$ toward $\bar{H}(m)$, $\bar{Q}^*(o_j)$ could be re-written as $\bar{Q}^*(o_j) = Q^\perp(o_j) + \cos \theta_{o_j} \cdot \bar{H}_m$, where $Q^\perp(o_j)$ is the auxiliary vector orthogonal to vector \bar{H}_m .

Then we plug the decomposed Q vectors $\bar{Q}^*(o_j)$ into the return gap we got in Eq.(20), the first part of the last step of Eq.(20) is bounded by:

$$\begin{aligned}
& \sum_{o_j \sim m} \bar{d}_m(o_j) \cdot \Phi_{max}(\bar{Q}^*(o_j)) \\
&= \sum_{o_j \sim m} \bar{d}_m(o_j) \cdot \Phi_{max}(Q^\perp(o_j) + \bar{H}(m) \cdot \cos \theta_{o_j}), \\
&\leq \sum_{o_j \sim m} \bar{d}_m(o_j) \cdot [\Phi_{max}(Q^\perp(o_j)) + \Phi_{max}(\bar{H}(m) \cdot \cos \theta_{o_j})], \\
&\leq \sum_{o_j \sim m} \bar{d}_m(o_j) \cdot [\Phi_{max}(Q^\perp(o_j)) + \Phi_{max}(\bar{H}(m))].
\end{aligned} \tag{23}$$

We use $\|\alpha\|_2$ to denote the L-2 norm of a vector α . Since the maximum function $\Phi_{max}(Q^\perp(o_j))$ can be bounded by the L_2 norm $C \cdot \|Q^\perp(o_j)\|_2$ for some constant C . We define a constant Q_{max} as the maximum absolute value of $\bar{Q}^*(o_j)$ in each cluster as $Q_{max} = \max_{o_j} \|\bar{Q}^*(o_j)\|_2$. Since $Q^\perp(o_j) = \bar{Q}^*(o_j) \cdot \sin(\theta)$, and $|\sin(\theta)| = \sqrt{1 - \cos^2(\theta)} = \sqrt{1 - [1 - \epsilon(o_j)]^2}$, the maximum value of $Q^\perp(o_j)$ could also be bounded by Q_{max} , i.e.:

$$\begin{aligned}
& \Phi_{max}(Q^\perp(o_j)) \leq C \cdot \|Q^\perp(o_j)\|_2, \\
& \leq C \cdot \|\bar{Q}^*(o_j)\|_2 \cdot |\sin \theta|, \\
& = C \cdot Q_{max} \cdot \sqrt{1 - [1 - \epsilon(o_j)]^2}, \\
& \leq O(\sqrt{\epsilon(o_j)} Q_{max}).
\end{aligned} \tag{24}$$

Plugging Eq.(24) into Eq.(23), we have:

$$\begin{aligned}
& \sum_{o_j \sim m} \bar{d}_m(o_j) \cdot \Phi_{max}(\bar{Q}^*(o_j)) \\
& \leq \sum_{o_j \sim m} \bar{d}_m(o_j) \cdot [\Phi_{max}(Q^\perp(o_j)) + \Phi_{max}(\bar{H}(m))], \\
& \leq \sum_{o_j \sim m} \bar{d}_m(o_j) \cdot [O(\sqrt{\epsilon(o_j)} Q_{max}) + \Phi_{max}(\bar{H}(m))], \\
& = \sum_{o_j \sim m} \bar{d}_m(o_j) \cdot [O(\sqrt{\epsilon(o_j)} Q_{max}) + \Phi_{max}(\bar{H}(m))],
\end{aligned} \tag{25}$$

It is easy to see from the last step in Eq.(20) that the return gap $J(\pi_{(j)}^*) - J(\pi_{(j)}, g)$ is bounded by the first part $\sum_m d_\mu^\pi(m) [\sum_{o_j \sim m} \bar{d}_m(o_j) \cdot \Phi_{max}(\bar{Q}^*(o_j))]$ which has an upper bound derived in

Eq.(25), then the return gap could also be bounded by the upper bound in Eq.(25), i.e.,

$$\begin{aligned}
& J(\pi_{(j)}^*) - J(\pi_{(j)}, g) \\
&= \sum_m d_\mu^\pi(m) \left[\sum_{o_j \sim m} \bar{d}_m(o_j) \cdot \Phi_{max}(\bar{Q}^*(o_j)) - \Phi_{max} \left(\sum_{o_j \sim m} \bar{d}_m(o_j) \cdot \bar{Q}^*(o_j) \right) \right], \\
&= \sum_m d_\mu^\pi(m) \left[\sum_{o_j \sim m} \bar{d}_m(o_j) \cdot [O(\sqrt{\epsilon(o_j)Q_{max}}) + \Phi_{max}(\bar{H}(m))] \right] - \sum_m d_\mu^\pi(m) \left[\Phi_{max} \left(\sum_{o_j \sim m} \bar{d}_m(o_j) \cdot \bar{Q}^*(o_j) \right) \right], \\
&\leq \sum_m d_\mu^\pi(m) \cdot \left[\sum_{o_j \sim m} \bar{d}_m(o_j) \cdot O(\sqrt{\epsilon(o_j)Q_{max}}) \right], \\
&\leq \sum_m d_\mu^\pi(m) \cdot O \left(\sqrt{\sum_{o_j \sim m} \bar{d}_m(o_j) \cdot \epsilon(o_j)Q_{max}} \right), \\
&\leq \sum_m d_\mu^\pi(m) \cdot O(\sqrt{\epsilon}Q_{max}), \\
&= O(\sqrt{\epsilon}Q_{max}).
\end{aligned} \tag{26}$$

we can derive the desired upper bound $J(\pi_{(j)}^*) - J(\pi_{(j)}, g) \leq O(\sqrt{\epsilon}Q_{max})$ for the two policies in Lemma 4.2 in the main paper. \square

C.3 Detailed process of calculation of the average cosine distance defined in Eq.(6) in the main paper

- Within each cluster, we compute the cosine distance between every action-value vector and the clustering center, thereby obtaining the value $\epsilon(o_j)$.
- To obtain the expectation of the cosine distance for each particular cluster denoted by m , we compute the product of each $\epsilon(o_j)$ with $\bar{d}_m(o_j)$, where $\bar{d}_m(o_j)$ represents the marginalized probability of o_j in cluster m .
- Having computed the expected cosine distance for each cluster m , we proceed to obtain the average cosine distance across all clusters. This is accomplished by multiplying $d_\mu^\pi(m)$ to each $\sum_{o_j \sim m} \bar{d}_m(o_j) \cdot \epsilon(o_j)$, where $d_\mu^\pi(m)$ denotes the visitation probability of message m .

C.4 Detailed Explanations for the Illustrative example

We want to use the example to illustrate the key intuitions behind our theoretical derivations, i.e., why the return gap in MARL with communications can be upper bounded by a term involving the average cosine distance ϵ .

The left figure in Fig.1 shows a centralized action-value(Q) table of a simple two-agent matrix game where the transition probability of the observations does not depend on policies and all observations are equally likely for each agent. The observation spaces are $\Omega_1 = \{o_{11}, o_{12}\}$ and $\Omega_2 = \{o_{21}, o_{22}, o_{23}, o_{24}\}$. Both agents have discrete action space, where $\mathcal{A}_1 = \{a_{11}, a_{12}\}$ and agent 2 has a deterministic policy to choose its actions based on its observation. $\bar{Q}^*(o_{2i})$ is the centralized action-value function vectors for each fixed o_{2i} , for example, the first column of Q vectors is $\bar{Q}^*(o_{21}) = [53.2, 42.9, 31.8, 22.9]$. The goal of the two agents is to maximize the average return which could be achieved by trying to take actions to maximize the centralized Q values.

In a partially observable environment where agents can only see their own observations, if agent 1 observes o_{11} , the average Q values of taking action a_{11} is $(53.2 + 4.5 + 58.5 + 0.3)/4 = 29.125$, which is smaller than $(42.9 + 1.2 + 64.0 + 16.1)/4 = 31.05$ by taking action a_{12} , so agent 1 will take action a_{12} and get the average return 31.05. Same calculations for observing o_{12} , then the agent 1 will get the total average return for two possible observations as $(31.05 + 35.6)/2 = 33.325$ with partial observation. In this situation, the agent 1 tries to choose the actions maximizing the Q values based on the average reward information, but since agent 1 does not know the observation of agent 2, it could not always choose the best action and result in some loss of average returns.

In a fully observable environment where agents can see others' observations, agent 1 could choose actions to maximize the Q values (shown as the bold numbers) which could be located by observations of both agents. The agent 1 will get the largest average reward as $(53.2 + 4.5 + 64.0 + 16.1)/4 = 34.425$ when observing o_{11} , and get $(31.8 + 28.0 + 34.1 + 81.5)/4 = 43.85$ when observing o_{12} , then the total average returns is $(34.425 + 43.85)/2 = 39.1375$.

The idea of our communication algorithm is to cluster the four observations of agent 2 which are invisible to agent 1 into 2^n clusters and send the cluster labels as a n -bit communication message to agent 1. Here we start with $n = 1$, i.e., only use 1-bit message in this example. The most important message agent 2 wants to send is where is the largest Q value located based on its own observation. Therefore, we use cosine distance $1 - \cos(\theta)$ as the clustering metric which is defined as the 1 abstract the cosine of angle θ between two vectors and two vectors with similar directions(smaller angle θ) have a smaller cosine distance. In this way, this clustering method could put the Q vectors with similar structures into the same cluster. We define the $\bar{Q}^*(o_{2i})$ as the centralized action-value function vectors for each fixed o_{2i} , for example, the Q vectors of fixed observation o_{21} of agent 2 is $\bar{Q}^*(o_{21}) = [53.2, 42.9, 31.8, 22.9]$.

Then we calculate the cosine distance between all possible pairs of Q vectors of agent 2 – $\bar{Q}^*(o_{2i})$ and $\bar{Q}^*(o_{2j})$, $\forall i, j \in \{1, 2, 3, 4\}$ and list the cosine distance between each pair in the right figure in Fig.1. Based on the cosine distance values, we put vectors with smaller cosine distance between them into the same cluster. For example, as for the observations of agent 2 which are unknown to agent 1, we put o_{21}, o_{23} into the same cluster and o_{22}, o_{24} into another cluster and use clustering labels 0, 1 respectively as communication messages being sent to agent 1. When agent 1 observes o_{11} and receive communication messages 0 from agent 2, it will know that agent 2 observes o_{21} or o_{23} , it will take action a_{11} not taking the a_{12} as it acted with only local observation, this is because $53.2 + 58.5 = 117.5$ is larger than $42.9 + 64.0 = 106.9$. Same as observing o_{11} and getting label 1, agent 1 will take action a_{12} since $1.2 + 16.1 = 17.3$ is larger than $4.5 + 0.3 = 4.8$, then the average return when agent 1 observing o_{11} becomes $(117.5 + 17.3)/4 = 33.7$. We do the same calculations when agent 1 observes o_{12} and get the average return as 43.85, then the total average returns for all conditions of agent 1 is $(33.7 + 43.85)/2 = 38.775$.

Therefore, the regret between policies with our method and the full observation is $39.1375 - 38.775 = 0.3625$, and the regret between policies with partial observation and full observation is $39.1375 - 33.325 = 5.8125$. We could see that using clustering labels as communication messages leads to a better decision with a small regret. And this clustering method not only works with discrete observation space but also could be compatible with any online clustering algorithm in order to use it with a continuous state space environment. In addition, the centralized Q table is available using centralized training decentralized execution algorithms mentioned in Section 2.

D RGMComm algorithm for n agents

D.1 RGMComm message generation training process

The message generation training process of our proposed Return-Gap-Minimization Communication(RGMComm) algorithm is summarized here in Algorithm 1, we also provide a complete pseudo-code for training later.

Algorithm 1 Training message generation

- 1: **Input:** K_1, K_2 , Replay buffer \mathcal{R} , current parameters ω, ξ .
 - 2: **for** $t = 1$ to T **do**
 - 3: **for** agent i to n **do**
 - 4: Get top- K_1 samples $\mathcal{S} = (\sigma^j, \mathbf{a}^j, R^j, \sigma'^j)$ from reply buffer \mathcal{R} ;
 - 5: Get top- K_2 samples $\mathcal{X}_{-i} = \{\sigma_{-i}, \mathbf{a}_{-i}\}$ from \mathcal{S} ;
 - 6: Combining (o_i, a_i) in \mathcal{S} and \mathcal{X}_{-i} as $\mathcal{D} = (\sigma^p, \mathbf{a}^p, R^p, \sigma'^p)$;
 - 7: Query the critic ω and get $\bar{Q}_\omega(o_i, \sigma_{-i}, a_i, \mathbf{a}_{-i})$;
 - 8: Update g_{ξ_i} by minimizing the loss using Eq.(13) in the main paper;
 - 9: **end for**
 - 10: **end for**
 - 11: **Output:** Message functions: $m_i = g_{\xi_i}(o_i)$.
-

D.2 RGMComm - Complete Training Pseudo-code

The complete training procedure of RGMComm algorithm is summarized in Algorithm 2 below.

Algorithm 2 RGMComm training Algorithm

- 1: **Input:** sampling size K_1 , K_2 , replay buffer size R , exploration constant τ_1, τ_2, τ_3 , learning rate $\alpha_0, \beta_0, \eta_0$;
 - 2: Initialize network weights (θ, ω, ξ) for each agent i at random;
 - 3: Initialize target weights $(\theta', \omega', \xi') \leftarrow (\theta, \omega, \xi)$ for each agent i at random;
 - 4: **for** episode= 1, 2, ..., **max-episode** **do**
 - 5: Start a new episode;
 - 6: Initialize a random process \mathcal{N} for action exploration;
 - 7: Receive initial observation $\mathbf{o} = [o_1, \dots, o_n]$;
 - 8: **for** $t = 1$ to **max-episode-length** **do**
 - 9: for each agent i , receive initial observation o_i , receive initial labels $m_{-i} = \{g_{\xi_j}(o_j), \forall j\}$;
 - 10: Generating communication labels $m_i = g_{\xi_i}(o_i)$;
 - 11: Select action $a_i = \pi_{\theta_i}(o_i, m_{-i}) + \mathcal{N}_t$ w.r.t. the current policy and exploration;
 - 12: Execute actions $\mathbf{a} = [a_1, \dots, a_n]$, observe reward R , new observation \mathbf{o}' ;
 - 13: Store $(\mathbf{o}, \mathbf{a}, R, \mathbf{o}')$ in replay buffer \mathcal{R} ;
 - 14: **for** agent $i = 1$ to n **do**
 - 15: Sample top- K_1 samples $\mathcal{S} = (\mathbf{o}^j, \mathbf{a}^j, R^j, \mathbf{o}'^j)$ from replay buffer \mathcal{R} ;
 - 16: Sample top- K_2 samples $\mathcal{X}_{-i} = \{\mathbf{o}_{-i}, \mathbf{a}_{-i}\}$ from \mathcal{S} ;
 - 17: Combining (o_i, a_i) in \mathcal{S} and \mathcal{X}_{-i} as $\mathcal{D} = (\mathbf{o}^p, \mathbf{a}^p, R^p, \mathbf{o}'^p)$;
 - 18: Query Centralized Critic parameterized by ω , and get K_1 vectors $\hat{Q}_\omega(o_i^p, \mathbf{o}_{-i}^p, a_i^p, \mathbf{a}_{-i}^p)$, each has a length of K_2 ;
 - 19: **for** $p = 1$ to K_1 **do**
 - 20: Normalize $\hat{Q}_\omega(o_i^p, \mathbf{o}_{-i}^p, a_i^p, \mathbf{a}_{-i}^p)$ and go through activation function f ;
 - 21: **end for**
 - 22: Getting the set of j nearest neighbors of each $\hat{Q}_\omega(o_i^p, \mathbf{o}_{-i}^p, a_i^p, \mathbf{a}_{-i}^p), \forall p$;
 - 23: Saving j nearest neighbors in set $N_j(p) = \{\hat{Q}_\omega(o_i^q, \mathbf{o}_{-i}^q, a_i^q, \mathbf{a}_{-i}^q), q = 1, \dots, j\}$
 - 24: Update g_{ξ_i} by minimizing the loss in using Eq.(13) in the main paper;
 - 25: Set $y^p = R^p + \gamma \hat{Q}_{\omega'}(\mathbf{o}'^p, \mathbf{a})|_{\mathbf{a}'=\pi'(\mathbf{o}'^p)}$;
 - 26: Update critic by minimizing the loss $\mathcal{L}(\omega) = \frac{1}{K_1} \sum_p [(\hat{Q}_\omega(\mathbf{o}^p, \mathbf{a}^p) - y^p)^2]$
 - 27: Update actor using the sampled policy gradient:
$$\nabla_{\theta_i} J(\theta_i) \approx \frac{1}{K_1} \sum_p \left[\nabla_{\theta_i} \log \pi_{\theta_i}(a_i | o_i^p, m_{-i}) \hat{Q}_\omega^{\pi_{\theta_i}}(\mathbf{o}^p, \mathbf{a}_1^p, \dots, a_i, \dots, \mathbf{a}_n^p) |_{a_i=\pi_{\theta_i}(o_i^p, m_{-i})} \right].$$
 - 28: Update actor network parameters: $\theta \leftarrow \theta + \alpha_t \delta_\theta$;
 - 29: Update critic network parameters: $\omega \leftarrow \omega + \beta_t \delta_\omega$;
 - 30: Update communication network parameters: $\xi \leftarrow \xi + \eta_t \delta_\xi$;
 - 31: **if** UPDATE TARGET NETWORKS **then**
 - 32: Update actor target network parameters:
$$\theta' \leftarrow \tau_1 \theta + (1 - \tau_1) \theta'$$
 - 33: Update critic target network parameters:
$$\omega' \leftarrow \tau_2 \omega + (1 - \tau_2) \omega'$$
 - 34: Update communication target network parameters:
$$\xi' \leftarrow \tau_3 \xi + (1 - \tau_3) \xi'$$
 - 35: **end if**
 - 36: **end for**
 - 37: **end for**
 - 38: **end for**
-

E Evaluations

E.1 Environment Details

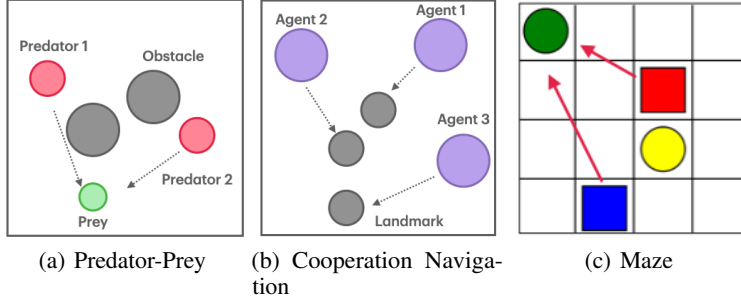


Figure 9: (a) and (b): Illustrations of the multi-agent particle environment in the experiments: Predator-Prey, Cooperative Navigation respectively. (c): Maze environment for the message-interpretation study.

Predator-Prey: This task involves a slower-moving team of N communicating predators (modeled as the learning RGMComm agents) chasing K faster moving preys in an environment with L obstacles. Each predator only gets its own local observation and a limited view of its nearest preys and obstacles without knowing other predators’ positions and velocities. Each time a predator collides with a prey, the predator is rewarded with $+10$ while the prey is penalized with -10 . The predators are also given a group reward $-0.1 \cdot \sum_{n=1}^N \min\{d(\mathbf{p}_n, \mathbf{q}_k), k \in \{1, \dots, K\}\}, n \in \{1, \dots, N\}$, where the \mathbf{p}_n and \mathbf{q}_k are the coordinates of predator n and prey k . The reward of the predators will be decreased for increased distance from preys.

Cooperative Navigation: In this environment, N agents need to cooperate to reach L landmarks while avoiding collisions. Each agent predicts the actions of nearby agents based on its own observation and received information from other agents. The agents are penalized if they collide with each other, and positively rewarded based on the proximity to the nearest landmark.

Maze Task: This is a simple tabular-case multi-agent task. Consider a 4 by 4 grid world in Fig.(9(c)), where landmark 1 (the green dot) with a high reward of r_1 is always placed at the higher left corner (1,1), while landmark 2 (the yellow dot) with a low reward of r_2 is always placed at the third diagonal position (3,3). Two agents (the red and the blue square) are randomly placed on the map and can only see their own position without seeing the targets’ positions or each other’s positions. There is no collision or movement cost. The task is completed and the reward r_1 (or r_2) is achieved only if both agents occupy the same landmark 1 (or 2) before or at the end of the game. Otherwise, zero rewards are achieved. The game terminates in 3 steps or when the task is completed.

E.2 Hyperparameters

In our experiments, the actor and critic neural networks consist of three hidden layer with 64 neurons and the Tanh activation function for actor, ReLU activation function for critic. For communication, the communication network has two hidden layers with 1200 units and use ReLU activation function. We use Adam optimizer with the learning rate of the actor-network as 0.0001, while the critic network has a learning rate of 0.001. This small difference makes the critic network learn faster than the actor-network. A slower learning rate of the actor could allow it to obtain feedback from the critic in each step, making the learning process more robust. For the soft update of target networks, we use $\tau = 0.01$. Finally, we use $\gamma = 0.95$ in the critic network to discount the reward and calculate the advantage functions. For the activation function $f((\bar{Q}^*(o_i^p) - \alpha)/\beta)$ in clustering metric, we use Tanh function as $f(\cdot)$ and $\alpha = (\max\{\bar{Q}^*(o_i^p)^1, \dots, \bar{Q}^*(o_i^p)^{K_1}\} + \min\{\bar{Q}^*(o_i^p)^1, \dots, \bar{Q}^*(o_i^p)^{K_1}\})/2$, $\beta = \max\{\bar{Q}^*(o_i^p)^1, \dots, \bar{Q}^*(o_i^p)^{K_2}\}$ to do the normalization, respectively.